PRAMANA
—journal of
physics

© Printed in India

Vol. 48, No. 1,
January 1997
pp. 249–258

Characterization and control of chaotic dynamics in a nerve conduction model equation

S RAJASEKAR
Department of Physics, Manonmaniam Sundaranar University, Tirunelveli 627 002, India

Abstract. In this paper we consider the Bonhoeffer–van der Pol (BVP) equation which describes propagation of nerve pulses in a neural membrane, and characterize the chaotic attractor at various bifurcations, and the probability distribution associated with weak and strong chaos. We illustrate control of chaos in the BVP equation by the Ott–Grebogi–Yorke method as well as through a periodic instantaneous burst.

Keywords. Bonhoeffer–van der Pol oscillator; local Lyapunov exponent; weak and strong chaos; controlling of chaos.

PACS Nos 05.45; 42.50

1. Introduction

During the last decade or so remarkable progress has been made in exploring the complexity of nonlinear systems, where the presence of chaos and other related phenomena have been extensively investigated [1, 2]. Particularly, routes to chaos, characterization of periodic and chaotic motions, multifractal, fractal basin boundary structures, etc. have been well established. In recent years there have been increasing interests in the study of

(i) statistical dynamics of local expansion rates [3–8],
(ii) characterization of chaotic attractors at bifurcations [9–14],
(iii) characterization of weak and strong chaos [15, 16],
(iv) controlling of chaos [2, 17–39] and
(v) synchronization of chaotic trajectories [2, 40–45].

1.1 *Local expansion rates and characterization of chaotic attractors at bifurcations*

Recently, the features associated with the fluctuations of local expansion rates of various attractors and statistical dynamics of local Lyapunov exponents have been studied [3–14]. Chaotic attractors have various local structures depending on their routes of onset and evolution. For instance, chaotic attractors are generally non-hyperbolic and have local homoclinic tangency structures. Bifurcations of chaos change the structures of chaotic attractors drastically and produce the coherent large fluctuations of the coarse-grained expansion rates Λ about the positive Lyapunov exponent λ. The q-weighted average $\Lambda(q)$

and the variance $\sigma_n(q)$ of fluctuations of $\wedge_n(x_1)$ around $\wedge_n(q)$ are useful for describing the coherent large fluctuations at the bifurcations of chaos.

1.2 *Weak and strong chaos*

In the literature, chaotic motion with small positive Lyapunov exponent is called weak chaos and chaotic motion with sufficiently large positive Lyapunov exponent is termed as strong chaos. Recently, Chen and Chow [15] have shown that weak and strong chaos can be characterized using probability distribution of k-step difference of a variable of the given dynamical system.

1.3 *Controlling of chaos*

Even though the presence of chaotic behaviour is generic and robust there are practical situations where one wishes to avoid or control chaos so as to improve the performance of a dynamical system. The ability to control chaos that is to convert chaotic oscillations into a desired regular ones with a periodic time dependence, would be beneficial in working with a particular system. Recently, more interest has been focussed on controlling of chaos and various methodologies that control chaos [17–26, 33].

1.4 *Synchronization of chaotic trajectories*

An approach which is closely related to controlling of chaos is that of obtaining the phase space trajectory of a chaotic system synchronized with another chaotic trajectory [2, 40–45] which has practical applications in secure communication. Here, synchronization is obtained by setting some of the variables of the synchronizing system to the values of the desired trajectory. The remaining variables asymptotically synchronize with the desired values provided the subsystem Lyapunov exponents for these variables are negative.

Thus, there are many interesting topics in chaos theory which have received much attention during the last few years and many fascinating results have been found. We have carried out investigations in these directions with reference to certain discrete and continuous dynamical systems [8, 12–14, 16, 27–33]. The goal of the present paper is to study the salient features associated with some of the above aspects of chaos with reference to the Bonhoeffer–van der Pol (BVP) equation. The BVP oscillator is an interesting dynamical system of considerable physical and biological significance [46].

The plan of the paper is as follows. In § 2 we characterize the chaotic attractor at various bifurcations, using the variance $\sigma_n(q)$ of fluctuations of coarse-grained local expansion rates of nearby orbits. Next, the probability distribution $P(\Delta V_k)$, $k = 1, 2, \ldots$ of $\Delta V_k = V_{m+k} - V_m$ where $V_1, V_2, \ldots$ are the values of the variable V in the Poincaré map of the BVP system is investigated in § 3. A stationary $P(\Delta V_k)$ distribution is shown to occur for strong chaos while nonstationary $P(\Delta V_k)$ is observed for weak chaos. Then, in § 4 we consider the problem of controlling of chaos. We present a brief summary of previous results on controlling of chaos in the BVP system. We show the stabilization of

unstable periodic orbit (UPO) of BVP oscillator by the method of Ott–Grebogi–Yorke [17], and the suppression of chaos by an additional instantaneous burst. Finally, §5 contains summary and conclusions.

2. Characterization of chaotic attractors at bifurcations in the BVP oscillator

In this section we study the characterization of chaotic attractors at critical bifurcations with reference to the BVP equation [28,47,48] which describes the propagation of an electrical impulse or voltage pulse along the membranes of nerve cell:

$$\dot{V} = V - V^3/3 - R + A_0 + A_1 \cos t, \tag{1a}$$

$$\dot{R} = c(V + a - bR). \tag{1b}$$

The variable V can be seen as the electric potential across the cell membrane, while R is a so-called recovery variable in which dynamic aspects of the state of the membrane are aggregated. a, b, c are membrane radius, specific resistivity of the fluid and temperature factor respectively and $A_0 + A_1 \cos t$ is the membrane current.

For a chaotic orbit $\{X_n\}, n = 1, 2, \ldots$ generated by a two dimensional map, we define the coarse-grained expansion rates [9–11] as

$$\wedge_n(X_1) = (1/n) \sum_{m=1}^{n} \lambda(X_m), \tag{2}$$

where $\lambda(X_m)$ is the local expansion rate of nearby orbits at X_m along the unstable manifold. The values of $\wedge_n(X_1)$ for different X_1's are randomly distributed between minimum and maximum values. To describe the fluctuations of the local expansion rates we consider the partition function [9–11]

$$Z_n(q) = \langle \exp[-n(q-1) \wedge_n (X_1)] \rangle, (-\infty < q < \infty) \tag{3}$$

where $\langle \ldots \rangle$ denotes the long time average. The scaling exponents can be defined in terms of the partition function as

$$\phi_n(q) = -(1/n) \ln Z_n(q), \tag{4}$$

$$\wedge_n(q) = \mathrm{d}\phi_n(q)/\mathrm{d}q, \tag{5}$$

$$\sigma_n(q) = -\mathrm{d} \wedge_n (q)/\mathrm{d}q. \tag{6}$$

For the BVP oscillator $\lambda(X_m)$ along the unstable manifold at X_m is calculated in the Poincaré map. The dynamical structure functions $\wedge_n(q)$ and $\sigma_n(q)$ are calculated for a range of values of the control parameter A_1 about its critical values A_{1c} at which bifurcations such as sudden widening of a chaotic attractor, band merging and intermittency occur.

The parameters in (1) are fixed at $a = 0.7$, $b = 0.8$, $c = 0.1$, $A_0 = 0$. A band merging crisis is found to occur at $A_1 = A_{1m} \approx 1.28653$: as A_1 is decreased to A_{1m} three bands of a chaotic attractor merge to form a single band chaotic attractor. Figure 1a shows $\sigma_n(q)$ at $A_1 = 1.287$ far from A_{1m}, where we have used $n = 21$. The $\sigma_n(q)$ has a peak at $q = q_\alpha \approx 1.65$. $\sigma_n(q)$ just before the band merging is shown in figure 1b. The $\sigma_n(q)$ has two peaks at $q = q_\alpha \approx 2.4$ and $q = q_\beta \approx 0.4$. Two peaks are observed for A_1 values just

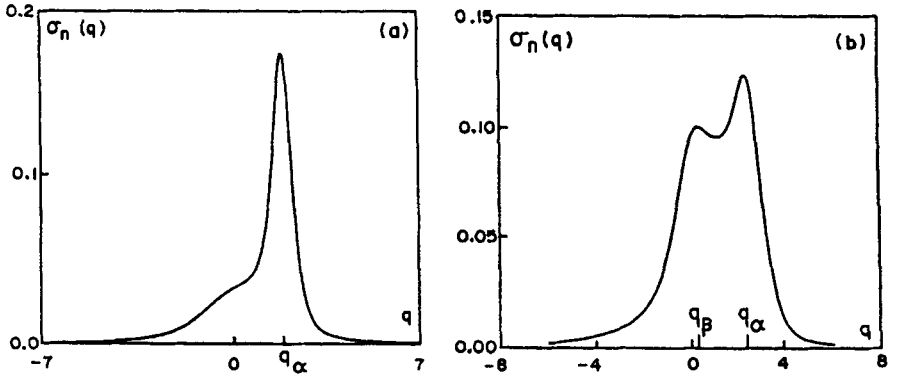

Figure 1. $\sigma_n(q)$ versus q for $A_1 = 1.287$ (**a**) far from band merging chaos and for $A_1 = 1.286$ (**b**) just before band merging chaos.

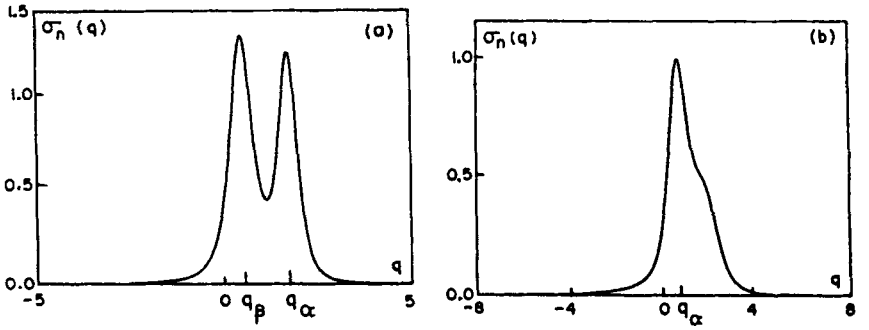

Figure 2. $\sigma_n(q)$ plots for (**a**) $A_1 = 1.0922$ in the intermittency region and (**b**) $A_1 = 1.096$ far after intermittency.

after the band merging also. For example, for $A_1 = 1.285$ peaks at $q_\alpha = 1.85$ and $q_\beta = -0.075$ are observed. Further, for $q = 1$, $\Lambda_n(1) = \Lambda^\infty$ and $\Lambda_n(\infty) = \Lambda_{\min}$ and $\Lambda_n(-\infty) = \Lambda_{\max}$. Therefore, $\sigma_n(q)$ with $q > 1$ and $q < 1$ can explicitly describe negative and positive large fluctuations of $\Lambda_n(X_1)$ respectively.

In the BVP equation, type I intermittent chaos is observed for $A_1 \in (1.092, 1.094)$. For A_1 values just below 1.092 a period-$4T(T = 2\pi)$ attractor is found. In the intermittency region the chaotic attractor has two types of local structures which produce the laminar and turbulent bursts respectively. Two types of local structures have been captured by the dynamical structure function $\sigma_n(q)$. Figure 2a shows $\sigma_n(q)$ versus q in the intermittency region. The A_1 value used is 1.0922 and $n = 10$. The $\sigma_n(q)$ has two peaks at $q = q_\alpha \approx 1.75$ and $q = q_\beta \approx 0.5$. Figure 2b shows the result for $A_1 = 1.096$ far after intermittency at which fully developed chaotic motion is observed. $\sigma_n(q)$ has only one peak at $q = q_\alpha \approx 0.6$.

A crisis, or sudden expansion in the size of the attractor is observed at $A = A_w \approx 0.747486$. For $A_1 = 0.73$, far from the crisis, $\sigma_n(q)$ has only one peak at $q = q_\alpha \approx 1.55$. Just before the crisis, corresponding to $A_1 = 0.747482$ the variance $\sigma_n(q)$ has two peaks at $q = q_\alpha \approx 2$ and $q_\beta \approx 0$.

From the above analysis we note that q_α peak is observed for all chaotic attractors. However, additional peaks in $\sigma_n(q)$ versus q plot occur just before and after the critical bifurcations. Thus it turns out that $\sigma_n(q)$ is useful for characterizing the chaotic attractors at bifurcations.

3. Characteristics of probability distribution in chaotic attractors of BVP oscillator

In this section we illustrate the characterization of weak and strong chaos in the BVP oscillator using the probability distribution of the k-step difference quantity of the variable V. Let $\{V_n\}, n = 1, 2, \ldots, N$ be the values of the variable V of (1) in the Poincaré map. We define the k-step difference quantity ΔV_k as $\Delta V_k = V_{m+k} - V_m$ where $m = 1, 2, \ldots, N', N' < N$. Then we calculate the probability distribution of ΔV_k.

Figure 3 shows the variation of maximal Lyapunov exponent (λ) as a function of A_1. In this plot there are many regions labelled by $\downarrow$, in which λ is positive but very small, indicating weak chaos. Distributions are calculated for various values of A_1. In numerical calculations we neglect the first 5000 Poincaré data as transient and use the next 10^4 points. For $A_1 = 1.0919$ the maximal Lyapunov exponent is ≈ 0.0004 and the corresponding chaotic motion is weak. For this A_1 value, P is found to change continuously with k. That is, the distribution is nonstationary. This is further verified by the chi-square, C^2 test quantity, defined as [15]

$$C^2(k,j) = \sum_{i=1}^{n} (R_i - S_i)^2/(R_i + S_i) \tag{7}$$

where R_i and S_i are the probabilities of the ith interval for $P(\Delta V_{k+j})$ and $P(\Delta V_k)$ respectively. In (7) intervals with $R_i = S_i = 0$ are excluded. If two probability distributions differ greatly, one gets a large C^2. For two similar distributions C^2 will be small. The numerically calculated C^2 is plotted in figure 4. The analysis is carried out for k values up to 5000. The nondecreasing C^2 implies the nonstationary characteristic of P. Thus, a complete probability distribution is impossible for weak chaos. A physical mechanism of nonstationary P can be a recurrence of memory loss and recovery of initial conditions [49].

Stationary probability distribution is found for strong chaos. For $A_1 = 1.26, \lambda$ is ≈ 0.056. The calculated C^2 is plotted in figure 5. For $k > 15$ C^2 is almost zero. That is,

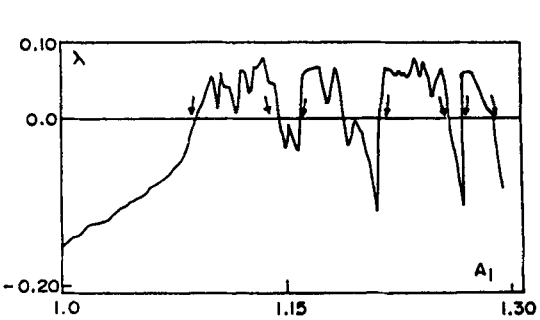

Figure 3. Estimated maximal Lyapunov exponent versus A_1.

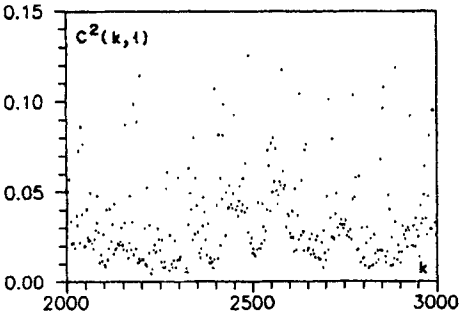

Figure 4. $C^2(k,1)$ versus k for the BVP chaotic attractor with $A_1 = 1.0919$ (weak chaos).

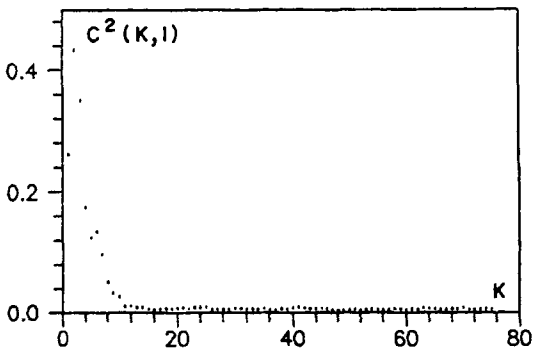

Figure 5. Same as figure (4) now for $A_1 = 1.26$ (strong chaos).

the distribution has evolved into a stationary state. This suggests that the variable V_n can be described as if it were generated by a random number generator with a certain probability distribution. A possible mechanism for a stationary distribution is complete loss of memory to the initial conditions. For two band and four band chaotic attractors, $C^2(k,1)$ values are found to be large (not shown). However, for two band and four band chaotic attractors $C^2(k,2)$ and $C^2(k,4)$ respectively decay to zero as k increases. Interestingly, for two (four) band attractor simple switching between two (four) different classes of P is found.

4. Controlling of chaos in the BVP equation

In this section we consider the problem of controlling of chaos in the BVP equation. First, we briefly review some previous results of controlling of chaos in the BVP equation.

4.1 *Previous results*

In a series of papers [27–33] we have studied the applicability and efficacy of a few control algorithms in the BVP equation.

Stabilization of UPO embedded in a chaotic attractor has been studied [28,29,31] by the control methods of Singer *et al* [21], Pyragas [22] and Chen and Dong [23]. A detailed comparative study of these methods has been made [31]. In all the three control schemes (i) stabilization of desired UPO is achieved for certain range of values of amplitude (ϵ) of the perturbation, (ii) before reaching the desired target the system exhibits transient evolution and (iii) the recovery time varies with the control strength ϵ.

Adaptive control algorithm [18, 19] with linear as well as nonlinear control functions is able to convert the chaotic attractors of the BVP system to a period-nT limit cycle [28,29]. Stable control is observed for certain range of values of stiffness (ϵ) of the control function. Further, the recovery time is found to be inversely proportional to ϵ.

We have investigated analytically [30] and numerically [28] the effect of periodic parametric perturbation and addition of second periodic force on chaotic dynamics. The period of the controlled motion is found to depend on amplitude and frequency of the added force. We have shown that most of the regular regime can be identified by the Melnikov method. Interestingly, suppression of chaos is found in the parametric regimes where the Melnikov function does not change sign.

4.2 *Ott–Grebogi–Yorke method*

In the OGY technique [17], stabilization of an UPO in a suitably defined Poincaré map can be achieved by slight adjustment of a control parameter. Suppose we wish to stabilize an unstable period-1 orbit contained in the chaotic attractor of BVP oscillator. We choose A_0 as the control parameter and denote $X_F(A_0 = 0)$ as the unstable period-1 orbit to be stabilized. As A_0 in (1) is varied slightly from $A_0 = 0$ to some $A_0 \neq 0$ then $X_F(0)$ will shift to $X_F(A_0)$. We define a vector g as $g = \partial X_F(A_0)/\partial A_0$ evaluated at $A_0 \neq 0$. Near $X_F(0)$ and for small values of A_0 one may write $\delta X_{n+1} \approx M\delta X_n$ where M is a 2×2 matrix and $\delta X_n = X_n - X_F(A_0)$. When the nth iteration X_n is close to X_F the value of A_0 is changed such that X_{n+1} falls on the stable manifold of X_F. That is, we choose the control δA_{0n} so that $f_u \cdot \delta X_{n+1} = 0$ which yields the control formula [17]

$$\delta A_{0n} = \frac{\lambda_u f_u \cdot \delta X_n}{(\lambda_u - 1) f_u \cdot g}, \tag{8}$$

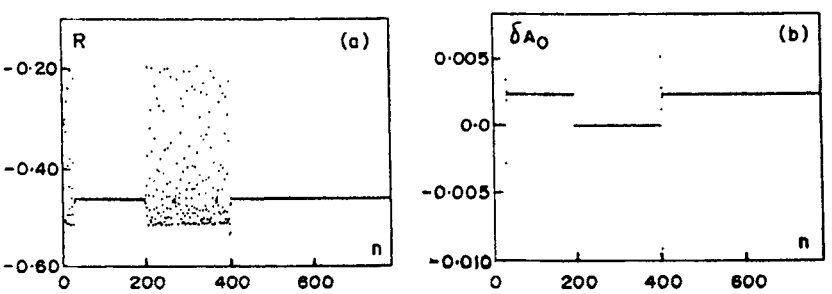

Figure 6. (a) The R-component of the period-1 orbit in the Poincaré map versus n. The control was switched on at $n = 30$, then switched off at $n = 200$ and then switched on at $n = 400$. (b) Perturbations δA_0 versus n.

where λ_u is the unstable eigenvalue of the matrix M and f_u is the unstable contravariant basis vector [17].

In the numerical simulation we found all pairs of iterates falling within the circles of radius 0.01 about the point $X_F(0)$. To this data we have fitted the approximate linear map and then determined the form of M and its eigenvalues and f_u. The approximate location of the period-1 unstable orbit is calculated as $X_F = (V_F, R_F) \approx (-0.9560, -0.4685)$. We have obtained $\lambda_u \approx 1.46, \lambda_s = -0.68, g \approx (0.105, 0.97)$ and $f_u = (1+\lambda_u^2)^{1/2}\,(\lambda_u - \lambda_s)^{-1}(1, \lambda_s)$. To stabilize the orbit X_F we have chosen the maximum allowed perturbation as $|\delta A_{0\max}| = 0.01$. Figure 6a illustrates the control of period-1 orbit. The period-1 orbit gets stabilized as long as the control is included. Figure 6b shows the perturbation δA_0 versus n.

4.3 *Suppression of chaos by periodic instantaneous burst*

The BVP equation with the addition of periodic instantaneous burst is written as [33]

$$\dot{V} = V - V^3/3 - R + A_1 \cos t, \tag{9a}$$

$$\dot{R} = c(V + a - bR) + \alpha g(t), \tag{9b}$$

where

$$g(t) = \sum_{n=1}^{\infty} \delta(t - n\tau T). \tag{9c}$$

The force $g(t)$ is nonzero and equal to unity only at times $t = n\tau T, n = 1, 2, \ldots$. For simplicity, T is fixed as 2π, period of the driving force. For fixed value of T the times at which $g(t)$ become nonzero and the period of the force are characterized by τ. Equation (9) is integrated using fourth order Runge–Kutta method with time step $2\pi/100$.

Figure 7 shows the bifurcation diagram as a function of α for $\tau = 0.5$. Chaotic behaviour persists for $\alpha \leq 0.0045$. Regular motion is recovered in the parameter interval $\alpha > 0.0045$. An interesting point here is the suppression of chaos by inverse period doubling phenomenon. Period $8T$, $4T$, $2T$ and T motions are found in the intervals (0.0051–0.0057), (0.006–0.0096), (0.0102–0.0309) and ($\alpha > 0.0312$) respectively. Next,

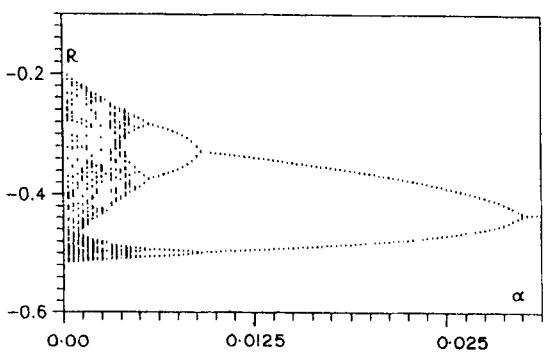

Figure 7. Bifurcation diagram of the BVP system (9). The parameters are fixed at $a = 0.7$, $b = 0.8$, $c = 0.1$, $A_1 = 0.74$, $T = 2\pi$ and $\tau = 0.5$.

α is kept at 0.006286 and τ is increased from small value in steps of 0.01 up to 1. Regular behavior is observed for $0.01 \leq \tau \leq 0.69$.

Further, the effect of phase difference ϕ between the periodic external force $A_1 \cos t$ and $g(t)$ is also studied. For various values of τ and α the dynamics of the BVP system is studied by varying ϕ. Interestingly, the behaviour of the system whether it is chaotic or periodic in the absence of ϕ is unaltered when ϕ is included. The only effect observed is an infinitesimal shift in the values of the state variables in the Poincaré map. A more detailed investigation of suppression of chaos by instantaneous burst will be presented elsewhere [33].

5. Summary and conclusions

In this paper we have studied various aspects of chaotic dynamics in the BVP oscillator. As shown for the BVP oscillator the chaotic attractors just near the critical bifurcations such as sudden widening, band merging and intermittency produce large fluctuations of the coarse-grained local expansion rates Λ, and consequently, additional peaks are found to occur in the $\sigma_n(q)$ versus q plot. On the other hand, a stationary probability distribution is found for chaotic attractors with large positive Lyapunov exponent, while for attractors with sufficiently small positive Lyapunov exponent a nonstationary probability distribution is observed. Thus, $\sigma_n(q)$ and $P(\Delta x_k)$ are useful to characterize various chaotic attractors.

We have discussed the problem of controlling of chaos in the BVP equation. If the aim is to set the system motion to a desired predetermined regular orbit, the adaptive control algorithm and feedback methods have distinct advantages. If one wishes to convert chaotic motion to some regular motion then periodic perturbations can be used. Surprisingly, chaotic motion can be suppressed by periodic kicks, which make the motion periodic.

References

[1] H G Schüster, *Deterministic chaos* (Verlag Chemie, Weinheim, 1988)
[2] M Lakshmanan and K Murali, *Chaos in nonlinear oscillators: controlling and synchronization* (World Scientific, Singapore, 1996)
[3] H D I Abarbanel, R Brown and M B Kennel, *J. Nonlinear. Sci.* **1**, 175 (1991)
[4] C Amitrano and R S Berry, *Phys. Rev.* **E47**, 3158 (1993)
[5] N Voglis and G J Contopoulos, *J. Phys.* **A27**, 4899 (1994)
[6] J L Chern and K Otsuka, *Phys. Lett.* **A188**, 321 (1994)
[7] S K Nayak, R Ramaswamy and C Chakravarty, *Phys. Rev.* **E51**, 3376 (1995)
[8] S Rajasekar, *Indian J. Phys.* **B70**, 51 (1996)
[9] R Ishizaki, T Horita and H Mori, *Prog. Theor. Phys.* **89**, 947 (1993)
[10] H Hate, T Horita and H Mori, *Prog. Theor. Phys.* **82**, 897 (1989)
[11] T Horita and H Mori, *Prog. Theor. Phys.* **91**, 677 (1994)
[12] S Rajasekar, *Phys. Rev.* **E52**, 3234 (1995)
[13] S Rajasekar, *Chaos, Solitons and Fractals* (1996, in press)
[14] P Philominathan and S Rajasekar, *Physica* **229**, 244 (1996)
[15] J L Chern and T C Chow, *Phys. Lett.* **A192**, 34 (1994)
[16] S Rajasekar, *Characteristics of probability distribution in chaos in an one dimensional map and BVP oscillator* (in preparation)

[17] E Ott, C Grebogi and J Yorke, *Phys. Rev. Lett.* **64**, 1196 (1990)
[18] B A Huberman and E Lumer, *IEEE Trans. Circuits Syst.* **37**, 547 (1990)
[19] S Sinha, R Ramaswamy and J Subba Rao, *Physica* **D43**, 118 (1990)
[20] R Lima and M Pettini, *Phys. Rev.* **A41**, 726 (1990)
[21] J Singer, Y Z Wang and H H Bau, *Phys. Rev. Lett.* **66**, 1123 (1991)
[22] K Pyragas, *Phys. Lett.* **A170**, 421 (1992)
[23] G Chen and X Dong, *Int. J. Bifur. Chaos* **2**, 407 (1992)
[24] Y Braiman and I Goldhirsch, *Phys. Rev. Lett.* **66**, 2545 (1991)
[25] A Hübler and E Luscher, *Naturwissenschaften* **76**, 67 (1989)
[26] E A Jackson, *Phys. Rev.* **A44**, 4839 (1991)
[27] S Rajasekar and M Lakshmanan, *Int. J. Bifur. Chaos* **2**, 201 (1992)
[28] S Rajasekar and M Lakshmanan, *Physica* **D67**, 282 (1993)
[29] S Rajasekar and M Lakshmanan, *J. Theor. Biol.* **166**, 275 (1994)
[30] S Rajasekar, *Pramana – J. Phys.*, **41**, 295 (1993)
[31] S Rajasekar, *Chaos, solitons and fractals*, **5**, 2135 (1995)
[32] S Rajasekar, *Phys. Rev.* **E51**, 775 (1995)
[33] S Rajasekar, *Controlling of chaos by periodic instantaneous burst* (submitted for publication)
[34] J K John and R E Amritkar, *Int. J. Bifur. Chaos* **4**, 1687 (1994)
[35] J K John and R E Amritkar, *Phys. Rev.* **E49**, 4843 (1994)
[36] K Murali and M Lakshmanan, *J. Circuits Systems and Computers* **3**, 125 (1993)
[37] S Parthasarathy and S Sinha, *Phys. Rev.* **E51**, 6239 (1995)
[38] S D Gadre and V S Varma, *Pramana – J. Phys.* **45**, 355 (1995)
[39] G Chen and X Dong, *Int. J. Bifur. Chaos* **3**, 1363 (1993)
[40] L M Pecora and T L Carroll, *Phys. Rev. Lett.* **64**, 821 (1990)
[41] R E Amritkar and Neelima Gupte, *Phys. Rev.* **A44**, 3403 (1991)
[42] Neelima Gupte and R E Amritkar, *Phys. Rev.* **E48**, R1620 (1993)
[43] R E Amritkar and Neelima Gupte, *Phys. Rev.* **E47**, 3889 (1993)
[44] K Murali and M Lakshmanan, *Phys. Rev.* **E48**, R1624 (1993)
[45] K Murali, M Lakshmanan and L O Chua, *Int. J. Bifur. Chaos* **5**, 563 (1995)
[46] A C Scott, *Neurophysics* (Wiley, New York, 1977)
[47] S Rajasekar and M Lakshmanan, *Physica* **D32**, 146 (1988)
[48] S Rajasekar, S Parthasarathy and M Lakshmanan, *Chaos, Solitons and Fractals* **2**, 271 (1992)
[49] P M Gade and R E Amritkar, *Phys. Rev.* **A45**, 725 (1992)